a reduction at $E_{p,c} = -1.23$ V vs. Ag/AgCl. An additional minor feature is present at $E_{p,c} = 0.69$ V. The corresponding potentials for **2** (Figure 6b) occur at values of +1.44 and -1.18 V. The relative inaccessibility of Rh_2^{3+} or Rh_2^{5+} core valencies in **1** and **2**, as evidenced by the high values of the redox potentials required to access them, implies that dppm and chloride ligands are quite effective in stabilizing the Rh_2^{4+} unit in the absence of μ-$O_2CCH_3^-$ groups.

Figure 7 shows three separate cyclic voltammograms of **3**. The initial scan direction is negative in Figure 7a, leading to the detection of two processes, both oxidations, at $E_{1/2} = 0.86$ V and $E_{p,a} = +1.24$ V vs. Ag/AgCl. In Figure 7b, the measurement was recorded in the same solution but with a reversal of scan direction. In this case there is an additional irreversible feature at $E_{p,c}$ -0.85 V due to a chemical product formed after compound **3** has been oxidized. The quasireversible couple at $E_{1/2} = +0.85$ V becomes more reversible and the product wave at -0.85 V disappears (Figure 7c) when the highest positive scan potential applied to the electrode is +1.10 V (instead of +1.50 V as in parts a and b). The accessibility of the reversible couple representing the process

$$Rh_2^{4+} \xrightarrow{-e^-} Rh_2^{5+}$$

suggests the feasibility of chemically isolating the cationic complex $[Rh_2Cl_2(dmpm)_2(Ph_2PC_6H_4)_2]^+$. Reactivity studies indicate that NO^+ is a suitable oxidizing agent for this purpose; further work is underway.

Conclusion. This work provides the basis for future investigations into dirhodium(II) chemistry with ligands other than small bidentate groups containing O-O or O-N donor atoms. The three new compounds reported here are significantly different than any previously known Rh_2^{4+} complexes. Furthermore, the geometry of the $Rh_2Cl_4(dppm)_2$ molecule constitutes a new structural type for $M_2X_4(L-L)_2$ species. Preliminary investigations into the reactivity of **1** and **3** imply that a rich chemistry is associated with chemical oxidation and removal of the axial chloride ligands. Compound **2**, although much more stable than **1** or **3**, appears to react with bases such as pyridine, but the products have not yet been identified.

Acknowledgment. We thank the National Science Foundation for support under Grant No. CHE-8514588. M.G.V. acknowledges the National Science Foundation of Belgium and the Fulbright Commission for support.

Supplementary Material Available: Full tables of bond distances, bond angles, and anisotropic displacement parameters for the crystal structures of **1**, **2**, and **3** (18 pages); tables of observed and calculated structure factors (52 pages). Ordering information is given on any current masthead page.

Synthesis and Characterization of Niobium(II) and Tantalum(II) Compounds Containing Triple M-M Bonds

F. Albert Cotton,* M. P. Diebold, and Wieslaw J. Roth

Contribution from the Department of Chemistry and Laboratory for Molecular Structure and Bonding, Texas A&M University, College Station, Texas 77843. *Received February 9, 1987*

Abstract: Convenient preparative methods for confacial bioctahedral dimers of Nb(II) and Ta(II) with a triple M-M bond of the formula $M_2X_6(THT)_3^{2-}$, where X = Cl or Br and THT = tetrahydrothiophene, have been developed. They involve reduction of $M_2X_6(THT)_3$ or MCl_5 with sodium amalgam in appropriate environments. Depending on the method of isolation, salts of different composition can be obtained and several of them have been characterized structurally. The following crystallographic data were obtained. $(NEt_4)_2[Nb_2Cl_6(THT)_3]\cdot CH_3CN$ (**1c**): space group $P\bar{1}$ with $a = 11.618$ (4) Å, $b = 19.226$ (4) Å, $c = 10.845$ (3) Å, $\alpha = 93.17$ (2), $\beta = 103.39$ (2)°, $\gamma = 107.70$ (3)°, $V = 2224$ (3) Å^3, and $Z = 2$; 324 parameters were refined to $R = 0.052$ and $R_w = 0.068$ with 5529 observables. $[Na(THF)_3]_2[Nb_2Cl_5(THT)_3]_2$ (**3**): space group $P2_1/n$ with $a = 13.649$ (4) Å, $b = 19.261$ (7) Å, $c = 14.112$ (4) Å, $\beta = 99.49$ (3)°, $V = 3659$ (2) Å^3, and $Z = 4$; 223 parameters were refined to $R = 0.0597$ and $R_w = 0.0702$ with 1582 observables. $[Na(THF)_3]_2[Nb_2Br_5(THT)_3]_2$ (**4**): space group $P\bar{1}$ with $a = 12.156$ (3) Å, $b = 16.098$ (7) Å, $c = 11.268$ (4) Å, $\alpha = 105.97$ (3)°, $\beta = 112.23$ (2)°, $\gamma = 95.68$ (3)°, $V = 1910$ (1) Å^3, and $Z = 2$; 343 parameters were refined to $R = 0.045$ and $R_w = 0.0566$ with 2360 observables. $[Li(THF)_2]_2[Ta_2Cl_6(THT)_3]$ (**5a**): space group $P\bar{1}$ with $a = 10.622$ (1) Å, $b = 22.468$ (3) Å, $c = 10.581$ (2) Å, $\alpha = 103.37$ (2)°, $\beta = 119.28$ (2)°, $\gamma = 83.31$ (2)°, $V = 2141$ (2) Å^3, and $Z = 2$; 236 parameters were refined to $R = 0.0612$ and $R_w = 0.0763$ with 3053 observables. $Na_2[Ta_2Cl_6(THT)_3]\cdot{}^3/_2THF$ (**5b**): space group $P2_1/n$ with $a = 11.044$ (2) Å, $b = 18.734$ (5) Å, $c = 16.019$ (5) Å, $\beta = 105.56$ (2)°, $V = 3193$ (1) Å^3, and $Z = 4$; 283 parameters were refined to $R = 0.0323$ and $R_w = 0.0457$ with 4019 observables. Spectroscopic characterization (UV-vis and proton NMR) has been carried out. MO calculations confirm the presence of a triple M-M bond and allow assignment of the electronic spectrum.

The field of metal-metal bonded complexes of the group 5 metals is rapidly growing. Many complexes containing single and double metal-metal bonds have been reported over the last few years. Complexes with double M-M bonds (M = Nb, Ta) have been synthesized by reduction of the pentahalides in the presence of donor ligands such as SMe_2,[1] THT (THT = tetrahydrothiophene),[2] PMe_3,[3] and PMe_2Ph.[4] The sulfur ligands give face-sharing bioctahedral complexes of the type $M_2X_6L_3$ whereas the phosphine ligands give edge-sharing bioctahedral species of the kind $M_2X_6L_4$. Both types of compounds have an extensive chemistry associated with them and have been used to form other

(1) (a) Allen, A. D.; Naito, S. *Can. J. Chem.* **1976**, *54*, 2948. (b) Cotton, F. A.; Najjar, R. C. *Inorg. Chem.* **1981**, *20*, 2716.

(2) (a) Mass, Jr.; E. T.; McCarley, R. E. *Inorg. Chem.* **1973**, *12*, 1096. (b) Templeton, J. L.; McCarley, R. E. *Inorg. Chem.* **1978**, *17*, 2293.

(3) Sattelberger, A. P.; Wilson, Jr., R. B.; Huffman, J. C. *J. Am. Chem. Soc.* **1980**, *102*, 7111.

(4) Hubert-Pfalzgraf, L.; Reiss, J. G. *Inorg. Chim. Acta* **1978**, *29*, L251.

0002-7863/87/1509-5506$01.50/0

niobium and tantalum complexes containing single or double M–M bonds.[1a,3,5] Compounds with single bonds are also formed by reducing the pentahalides with 1 equiv of reducing agent or by reacting monomeric $NbCl_4L_2$ (L = THF, CH_3CN) with ligands such as MeOH[6] or PMe_3.[7]

One major deficiency in this field is the paucity of complexes containing M–M triple bonds. This is especially surprising since group 6 metals readily form not only triple but also quadruple bonds.[8] For vanadium a few complexes containing V–V triple bonds have been made. Atwood et al. reported $(\eta^6\text{-}C_6H_6)_2V_2(CO)_4$ as a decomposition product of $V(CO)_6$.[9] A preliminary structure determination indicated that a V–V triple bond was present. Complexes of the type $V_2(DMP)_4$ and $V_2(TMP)_4$ (DMP = 2,6-dimethoxyphenyl, TMP = 2,4,6-trimethoxyphenyl)[10] have edge-sharing bioctahedral structures in which the metals participate in $\sigma^2\pi^2\delta^2$-type triple bonding.[11]

Until recently there has been a complete lack of niobium and tantalum complexes containing triple M–M bonds, which might be anticipated for these elements in their oxidation state +2. Although several M(II) compounds are known, most of them are monomeric. Dinuclear complexes of Nb and Ta in higher oxidation states are often not reducible by common reducing agents. For example, while $W_2Cl_6(PMe_3)_4$ can be reduced to form $W_2Cl_4(PMe_3)_4$, the tantalum analogue cannot.[3]

We have recently reported the synthesis and crystal structure of a tantalum dimer, $Ta_2Cl_6(\mu\text{-}THT)_3^{2-}$, containing a Ta–Ta triple bond.[12] This diamagnetic compound was made by the reduction of $Ta_2Cl_6(THT)_3$ in THF. Since that time we have generalized our procedure and have isolated the analogous niobium dimer as well as $Nb_2Br_6(\mu\text{-}THT)_3^{2-}$. We have also found that in THF the sodium salts of these complexes are unstable with respect to the formation of an insoluble red product which we have identified as the triple bond containing tetrameric complexes $[M_2X_5(\mu\text{-}THT)_3]_2^{2-}$. We now wish to report the characterization and general preparations of these triple-bonded complexes.

Experimental Section

All manipulations were carried out by using standard double-manifold vacuum line techniques under an atmosphere of argon. $TaCl_5$ and $NbCl_5$ were purchased from Pressure Chemicals, Inc., and Aesar, respectively, and used as received. $Ta_2Cl_6(THT)_3$,[2b] $Nb_2Cl_6(THT)_3$,[2a] and $Nb_2Br_6(THT)_3$[2a] were prepared according to literature methods. The spectra reported were recorded on the following instruments: UV–visible, Cary 17D spectrophotometer; ^1H NMR, Varian EM390 and XL-200 NMR spectrometers.

Preparation of $[Li(THF)_2]_2[Nb_2Cl_6(\mu\text{-}THT)_3]$ (1a). A. Reduction of $Nb_2Cl_6(THT)_3$. A mixture of $Nb_2Cl_6(THT)_3$ (0.66 g, 1.0 mmol) and LiCl (0.085 g, 2.0 mmol) were dissolved in 30 mL of THF. After a few minutes the solution became cloudy as $Nb_2Cl_6(\mu\text{-}THT)(THF)_2$ precipitated. Sodium amalgam (2.0 mmol of Na in 1.0 mL of Hg) was added, and the solution was stirred vigorously for 4 h. After standing for 15 min the dark red solution was decanted from the gray precipitate and filtered. The volume of the solution was reduced in vacuo to about 20 mL, and hexane was added until slight precipitation occurred (~25 mL). The solution was placed at −20 °C overnight, and the following day the precipitate was collected, washed with hexane, and dried in vacuo for several hours; yield 0.42 g, 62%. NMR showed slight variations in the amount of solvent THF present. UV–vis (THF): 508, 409 nm.

B. Reduction of $NbCl_5$. To a slurry of $NbCl_5$ (5.0 g, 18.5 mmol) and LiCl (0.78 g, 18.5 mmol) in 40 mL of toluene was added 3.1 mL (35.1 mmol) of THT and sodium amalgam (60.0 mmol of Na in 25 mL of Hg). The mixture was stirred with a mechanical stirrer for 2 h to give a purple solution ($Nb_2Cl_6(THT)_3$) and a gray precipitate. THF (100 mL) was syringed into the still stirring solution. The solution turned red within minutes but was allowed to react overnight. The following day, the solids were allowed to settle and the red solution was decanted into another flask. The solids were washed with 3 × 50 mL of THF. These washings were combined with the original solution and filtered through 2 cm of Celite. All but 70 mL of solvent was removed in vacuo, and 100 mL hexane was added to the solution with stirring. The resulting red precipitate was collected and washed with hexane until the washings were colorless. The solid was dried in vacuo for several hours; yield 5.98 g, 60%. Product free from the small amount of LiCl contamination still present could be obtained by recrystallization from THF/hexane.

Preparation of $Na_2[Nb_2Cl_6(\mu\text{-}THT)_3]\cdot n$THF (1b). This compound was prepared by omitting LiCl from either of the above preparations for **1a**. Compound **1b** was isolated in slightly lower yields than **1a** and the amount of solvent THF present in the solid, as determined by ^1H NMR, varied from sample to sample. Solutions of **1b** in THF clouded with time as compound **3** formed (vide infra). Compound **1b** had ^1H NMR and UV–vis spectra virtually identical with those of compound **1a**.

Preparation of $[Et_4N]_2[Nb_2Cl_6(\mu\text{-}THT)_3]$ (1c). To a slurry of $NbCl_5$ (5.4 g, 20 mmol) in 100 mL of benzene was added 4 mL of THT and sodium amalgam (1.5 g, 65 mmol in 15 mL of Hg). After the mixture had been stirred for several hours, the volume of the solution was reduced by approximately half. THF (100 mL) was added, and the contents of the flask were stirred overnight. The red-brown solution was decanted and the residue washed twice with 100 mL of THF. The combined liquids were filtered through Celite. NEt_4Cl (4.1 g, 25 mmol) was added, and upon stirring for 24 h a fine brown precipitate formed. It was isolated by filtration and redissolved in 60 mL of CH_3CN. The red solution was separated from a white solid by filtration and its volume reduced to about 10 mL. The first crop of brick red crystalline material (3.1 g) was isolated by filtration, washed with CH_3CN/THF (1:3), and dried under vacuum. The filtrate was evaporated to ca. 3 mL, and a second crop of the product was collected (1.3 g). The combined yield was 4.4 g, 45% based on Nb.

^1H NMR (CD_3CN, δ): 3.37 (α-CH_2 in THT; multiplet, 12 H), 3.18 (CH_2 in NEt_4^+; quartet, 16 H), 2.11 (β-CH_2 in THT; multiplet, 12 H), 1.97 (CH_3CN; singlet), 1.94 (CD_2HCN; quintet), 1.20 (CH_3 in NEt_4^+; triplet of triplets, 24 H). UV–vis (CH_3CN): 509, 406 nm.

Preparation of $Na_2[Nb_2Br_6(\mu\text{-}THT)_3]\cdot n$THF (2). Procedure A for **1a** was modified by using $Nb_2Br_6(THT)_3$ (1.0 mmol) in place of $Nb_2Cl_6(THT)_3$ and omitting the LiCl. Yields for **2** were about 50%. The UV–vis spectrum showed one maximum at 517 nm and a rapidly rising absorption peak beginning at ca. 420 nm.

Preparation of $[Na(THF)_3]_2[Nb_2X_5(\mu\text{-}THT)_3]_2$, X = Cl (3) or Br (4). Solutions of either **1b** (0.5 g) or **2** (0.25 g) in 20 mL of THF were left undisturbed at room temperature for several days. After this time the crystalline precipitate that formed was filtered and washed with THF to yield **3** or **4**, respectively.

Preparation of $[Li(THF)_2]_2[Ta_2Cl_6(\mu\text{-}THT)_3]$ (5a) and $Na_2[Ta_2Cl_6(\mu\text{-}THT)_3]\cdot n$THF (5b). These compounds were prepared by following the above procedures for the analogous niobium complexes using $TaCl_5$ or $Ta_2Cl_6(THT)_3$ as starting materials. Yields were somewhat lower for the tantalum complexes. ^1H NMR and UV–vis spectra were essentially identical for **5a** and **5b**.

^1H NMR (CD_3CN, δ): 3.55, 1.66 (THF); 3.00, 2.06 (μ-THT); 2.50, 1.69 (free THT; peaks were small).

X-ray Crystallography. Single-crystal X-ray analyses have been performed on $[NEt_4]_2[Nb_2Cl_6(\mu\text{-}THT)_3]$ (**1c**), $[Na(THF)_3]_2[Nb_2Cl_5(\mu\text{-}THT)_3]_2$ (**3**), $[Na(THF)_3]_2[Nb_2Br_5(\mu\text{-}THT)_3]_2$ (**4**), $[Li(THF)_2]_2[Ta_2Cl_6(\mu\text{-}THT)_3]$ (**5a**), and $Na_2[Ta_2Cl_6(\mu\text{-}THT)_3]\cdot{}^3/_2$THF (**5b**). The unit cell determinations and collections of intensity data were carried out by following procedures routine to this laboratory and described elsewhere in detail.[13] The structures were solved and refined by standard computational methods,[14] and no unusual problems were encountered. The data were corrected for Lorentz and polarization effects. Empirical

(5) (a) Clay, M. E.; Brown, T. M. *Inorg. Chim. Acta* **1983**, *72*, 75. (b) Cotton, F. A.; Hall, W. T. *Inorg. Chem.* **1980**, *19*, 2354. (c) Cotton, F. A.; Falvello, L. R.; Najjar, R. C. *Inorg. Chem.* **1983**, *22*, 375. (d) Cotton, F. A.; Diebold, M. P.; Matusz, M.; Roth, W. J. *Inorg. Chim. Acta* **1986**, *112*, 147. (e) Cotton, F. A.; Diebold, M. P.; Duraj, S. A.; Roth, W. J. *Polyhedron* **1985**, *4*, 1479. (f) Cotton, F. A.; Diebold, M. P.; Llusar, R.; Roth, W. J. *J. Chem. Soc., Chem. Commun.* **1986**, 1276. (g) Sattelberger, A. P.; Wilson, Jr., R. B.; Huffman, J. C. *Inorg. Chem.* **1982**, *21*, 4179.

(6) (a) Gut, R.; Perron, W. *J. Less Common Met.* **1972**, *26*, 369. (b) Cotton, F. A.; Diebold, M. P.; Roth, W. J., unpublished results.

(7) (a) Manzer, L. E. *Inorg. Chem.* **1977**, *16*, 525. (b) Cotton, F. A.; Roth, W. J. *Inorg. Chem.* **1984**, *23*, 945.

(8) Cotton, F. A.; Walton, R. A. *Multiple Bonds Between Metal Atoms*; Wiley: New York, 1982.

(9) Atwood, J. D.; Janik, T. S.; Atwood, T. L.; Rodgers, R. D. *Synth. React. Inorg. Met.-Org. Chem.* **1980**, *10*, 397.

(10) (a) Seidel, W.; Kreisel, G.; Menneng, H. *Z. Chem.* **1976**, *16*, 492. (b) Cotton, F. A.; Lewis, G. E.; Mott, G. N. *Inorg. Chem.* **1983**, *22*, 560.

(11) Cotton, F. A.; Diebold, M. P.; Shim, I. *Inorg. Chem.* **1985**, *24*, 1510.

(12) Cotton, F. A.; Diebold, M. P.; Roth, W. J. *J. Am. Chem. Soc.* **1986**, *108*, 3538.

(13) (a) Bino, A.; Cotton, F. A.; Fanwick, P. E. *Inorg. Chem.* **1979**, *18*, 3558. (b) Cotton, F. A.; Frenz, B. A.; Deganello, G.; Shaver, A. *J. Organomet. Chem.* **1973**, *50*, 227.

(14) Calculations were done on the VAX-11/780 computer at Department of Chemistry, Texas A&M University, College Station, TX, with the VAX-SDP software package.

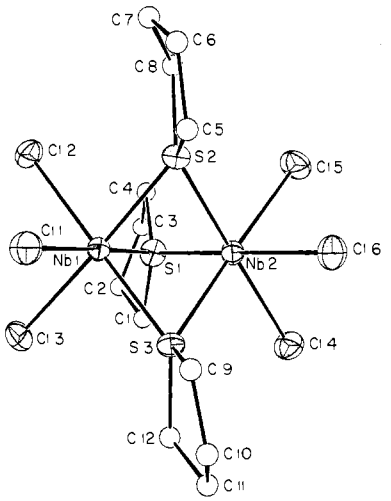

Figure 1. View of the anion in $[NEt_4]_2[Nb_2Cl_6(\mu\text{-}THT)_3]\cdot CH_3CN$ (**1c**). Non-carbon atoms are drawn at the 30% probability level; carbon atoms are shown as spheres of arbitrarily small radius.

absorption corrections based on azimuthal scan data were applied to all structures except **1c**, for which the method of Walker and Stuart[15] was used. Pertinent crystallographic information is summarized in Table I.

In all cases the positions of the metal atoms were derived by using standard procedures from three-dimensional Patterson maps. All non-hydrogen atoms were located through a series of difference Fourier syntheses and least-squares refinements. Anisotropic displacement parameters were assigned to selected atoms (see Tables II–VI) and the structures refined to convergence by full-matrix least-squares techniques.

For the tetraethylammonium salt **1c**, the alkyl groups in one of the cations were disordered about the nitrogen atom. After refinement of multiplicities of the carbon atoms located in the difference Fourier map, the fractional occupancies were set to 0.7 and 0.3 for C(21) through C(28) and C(21A) through C(28A), respectively. In most cases each terminal carbon atom gave reasonable distances and angles with two of the methylene carbon atoms. A molecule of solvent, CH_3CN, was also present interstitially. It was disordered as well, as shown by the residual electron density remaining around C(29) and C(30). Since the molecule was poorly defined and its interatomic dimensions were not accurate, the assignment of the nitrogen atom was made arbitrarily.

In compound **5b** a difference map revealed some electron density in a cavity located about an inversion center. A distorted THF ring, disordered about this inversion center and given half occupancy, was used to model this region. Although this model was not entirely accurate, as evidenced by anomalous carbon–carbon distances and angles and by a surfeit of electron density still present in that region of the difference Fourier map, it was deemed satisfactory for practical purposes and no attempt was made to improve on it. All other atoms were refined anisotropically.

Tables of observed and calculated structure factors and anisotropic displacement parameters are available as supplementary material.

Results and Discussion

Molecular Structures. Positional and isotropic-equivalent displacement parameters for **1c**, **3**, **4**, **5a**, and **5b** are presented in Tables II–VI, respectively. Important bond distances and angles are summarized in Tables VII–X. Complete listings of bond distances and angles are available as supplementary material. The common structural unit in all the compounds described here is the confacial bioctahedral dimer of formula $[M_2X_6(\mu\text{-}THT)_3]^{2-}$, a representative example of which is shown in Figure 1. In all cases two metal atoms are bridged by the sulfur atoms of three THT ligands, and each has three halide atoms completing the distorted octahedral coordination sphere. The metal–metal distances fall in a narrow range around 2.61 Å, indicating strong metal–metal bonding. The M–S–M bond angles average to 65.7°, considerably less than the value of 70.53° expected for an ideal confacial bioctahedron with no metal–metal interactions. This indicates strong metal–metal bonding as well. The metal to halogen distances are completely normal and seem to be little affected in the cases where the halogen atoms are also bound to the alkali metal counterion.

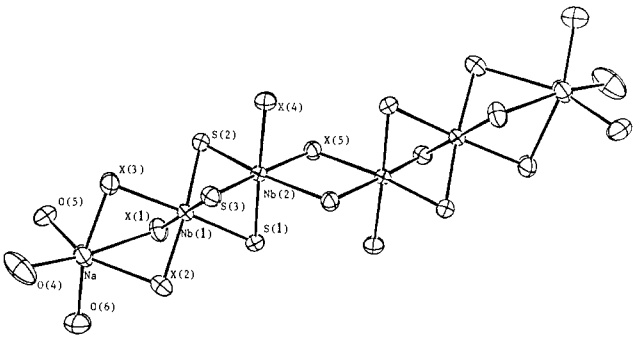

Figure 2. View of a representative $[Na(THF)_3]_2[Nb_2X_5(\mu\text{-}THT)_3]_2$ molecule (X = Cl, **3**; X = Br, **4**). Carbon atoms have been omitted for clarity.

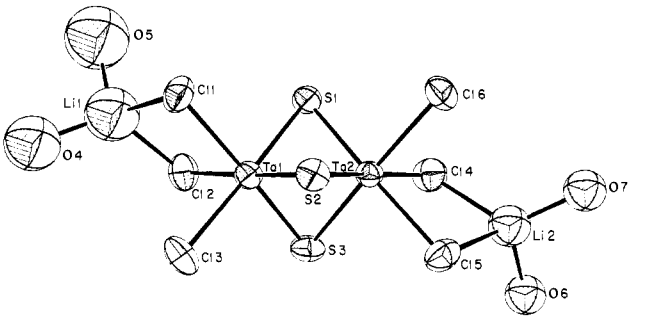

Figure 3. View of the $[Li(THF)_2]_2[Ta_2Cl_6(\mu\text{-}THT)_3]$ molecule (**5a**) drawn at the 30% probability level. Carbon atoms have been omitted for clarity.

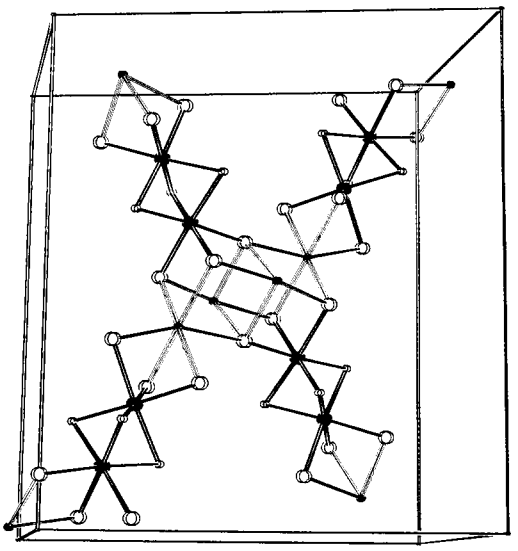

Figure 4. Unit cell packing diagram of $Na_2[Ta_2Cl_6(\mu\text{-}THT)_3]\cdot{}^3/_2THF$. Large open circles represent Cl atoms, small open circles represent S atoms, large filled circles represent Ta atoms, and small filled circles represent Na atoms. Carbon atoms on the THT rings and all THF molecules were omitted for clarity.

In compounds **3** and **4** two of these dinuclear units are joined to form a centrosymmetric tetramer, shown in Figure 2, with concomitant extrusion of two equivalents of NaX. The two outer metals on each side of the tetramer are in a face-sharing bioctahedral environment with respect to each other while the inner two metal atoms are in an edge-sharing bioctahedral environment with respect to each other. The outer two pairs of metal atoms are in much closer proximity to one another (~2.6 Å apart) than is the inner pair (>3.9 Å apart).

For the alkali-metal salts the ends of the anions interact strongly with the counterion. In **3**, **4**, and **5a** the counterion is bound to

(15) Walker, N.; Stuart, D. *Acta Crystallogr., Sect. A: Found. Crystallogr.* **1983**, *A39*, 158.

Table I. Crystal Data

	1c	3	4	5a	5b
formula	$Nb_2Cl_6S_3N_3C_{30}H_{67}$	$Nb_2Cl_5S_3NaO_3C_{24}H_{48}$	$Nb_2Br_5S_3NaO_3C_{24}H_{48}$	$Ta_2Cl_6S_3O_4C_{28}Li_2H_{56}$	$Ta_2Cl_6S_3Na_2O_{3/2}C_{18}H_{36}$
fw	964.61	866.91	1089.19	1141.43	993.22
space group	$P\bar{1}$	$P2_1/n$	$P\bar{1}$	$P\bar{1}$	$P2_1/n$
systematic absences		$0k0$, $k = 2n + 1$ $h0l$, $h + l = 2n + 1$			$0k0$, $k = 2n + 1$ $h0l$, $h + l = 2n + 1$
a, Å	11.618 (4)	13.649 (4)	12.156 (3)	10.622 (1)	11.044 (2)
b, Å	19.226 (4)	19.261 (7)	16.098 (7)	22.468 (3)	18.734 (5)
c, Å	10.845 (3)	14.112 (4)	11.268 (4)	10.581 (2)	16.019 (5)
α, deg	93.17 (2)	90.0	105.97 (3)	103.37 (2)	90.0
β, deg	103.39 (2)	99.49 (3)	112.23 (2)	119.28 (2)	105.56 (2)
γ, deg	107.70 (3)	90.0	95.68 (3)	83.31 (2)	90.0
V, Å^3	2224 (3)	3659 (2)	1910 (1)	2141 (1)	3193 (1)
Z	2	4	2	2	4
d_{calcd}, g/cm^3	1.440	1.574	1.894	1.770	2.070
cryst size, mm	0.1 × 0.3 × 0.4	0.25 × 0.25 × 0.10	0.2 × 0.3 × 0.05	0.3 × 0.3 × 0.2	0.6 × 0.5 × 0.35
μ(Mo Kα), cm^{-1}	10.161	11.683	59.470	55.953	78.157
data collecn instrument	CAD-4	Syntex P$\bar{1}$	Syntex P$\bar{1}$	Syntex P3	Syntex P3
radiatn (monochromated in incident beam)	Mo Kα (λ_α = 0.71073 Å)	Mo Kα (λ_α = 0.71073 Å)	Mo Kα (λ_α = 0.71073 Å)	Mo Kα (λ_α = 0.71073 Å)	Mo Kα (λ_α = 0.71073 Å)
orientatn reflectns; no., range (2θ)	25; 14.8°, 36.7°	15; 16.1°, 28.6°	15; 20.0°, 30.0°	25; 20.4°, 32.1°	23; 21.0°, 30.0°
temp, °C	22	6	6	22	22
data col range, 2θ, deg	$4.0 < 2\theta < 50.0$	$4.0 < 2\theta < 45.0$	$4.25 < 2\theta < 45.0$	$4.0 < 2\theta < 50.0$	$4.25 < 2\theta < 50.0$
no. unique data, total with $F_o^2 > 3\sigma(F_o^2)$	6778, 5529	2243, 1582	3583, 2360	4976, 3053	5368, 4019
no. of parameters refined	324	223	343	236	283
trans factors, max, min	1.0, 0.82	0.9996, 0.8846	0.9989, 0.4484	0.9995, 0.5130	0.9994, 0.8493
R^a	0.052	0.0597	0.0450	0.0612	0.0323
$R_w{}^b$	0.068	0.0702	0.0566	0.0763	0.0457
quality-of-fit indicator[c]	1.901	1.259	1.128	1.355	1.005
largest shift/esd, final cycle	0.19	0.25	0.08	0.16	0.60
largest peak, e Å^{-3}	0.927	0.610	0.736	1.221[d]	0.808

[a] $R = \sum||F_o| - |F_c||/\sum|F_o|$. [b] $R_w = [\sum w(|F_o| - |F_c|)^2/\sum w|F_o|^2]^{1/2}$; $w = 1/\sigma^2(|F_o|)$. [c] Quality-of-fit = $[\sum w(|F_o| - |F_c|)^2/(N_{obsd} - N_{parameters})]^{1/2}$. [d] Several peaks above 1.0 e Å^{-3} were located around the heavy atoms.

either two or three halogen atoms from the dimer and to THF molecules. The sodium cations are six-coordinate while the smaller lithium cations are four-coordinate (see Figure 3). In **5b** the sodium cation is bonded to the chlorine atoms in a more complicated manner, as shown in the unit cell packing diagram (Figure 4). Four dinuclear units are present per unit cell and are arranged so that one end of each unit is close to the center of the cell. These ends are then held together by the sodium counterions. There are two types of sodium atoms: one is coordinated to six chlorine atoms while the other is coordinated to four chlorine atoms and one molecule of THF (not shown in Figure 4). The angles about the sodium and chlorine atoms are close to 90°, and the region where four dinuclear units join together is similar to the lattice structure of rock salt. The joining of dinuclear units continues in all directions resulting in an extended three-dimensional array. A unit cell determination on $Na_2[Nb_2Cl_6(\mu\text{-THT})_3]\cdot n$THF (**1b**) shows it to be isomorphous with **5b**.

Synthesis. Complexes of Nb(II) and Ta(II) are relatively rare. Reduction of compounds containing these metals in higher oxidation states usually terminates with the formation of M(IV) or M(III) complexes, even when excess reducing agent is present. Only for certain combinations of solvent and ligand set can reduction to the +2 state be made. Most of these M(II) complexes are monomeric, octahedral species of the type MX_2L_4 (M = Nb, Ta; X = Cl; L = PMe_3 or $^1/_2$dmpe[16] and M = Nb; X = OAr; L = $^1/_2$dmpe[17]). Only two Nb(II)–Nb(II) dimers have been reported, namely, $(CpNb(CO)_2)_2(\mu\text{-Cl})_2$ and $(CpNb(PhCCPh))_2(\mu\text{-Cl})_2$.[18] The long M–M distances (~3 Å) in these compounds are consistent with single rather than triple metal–metal bonds. Ours are the first examples of M(II)–M(II) dimers containing triple M–M bonds.

Two distinct strategies might be envisioned for making M(II)–M(II) dimers. The first would be to start with monomeric complexes in which the metal atoms are in the proper (+2) oxidation state. Reacting these monomers with potentially bridging ligands could then lead to dimerization and metal–metal bond formation. The second strategy would be to attempt the reduction of already dinuclear compounds containing lower order (single or double) M–M bonds. Methods of both types have been used successfully to form quadruply bonded complexes of the group 6 metals.[8] Although work employing the first method has not yet succeeded for niobium and tantalum, this method may yet prove to be feasible if the right combination of monomeric starting material and bridging ligand is used. We have recently been concentrating our efforts on the second method. After trying to reduce several dimeric complexes with M–M double bonds, we found that $M_2X_6(\mu\text{-THT})(THF)_2$,[19] formed by dissolving $M_2X_6(THT)_3$ in THF, can be reduced smoothly and rapidly to produce the $M_2X_6(\mu\text{-THT})_3{}^{2-}$ complexes. It is the $M_2X_6(\mu\text{-THT})(THF)_2$, and not the $M_2X_6(THT)_3$, that is the key reactant since $M_2X_6(THT)_3$ cannot be reduced in toluene, yet $M_2X_6(\mu\text{-THT})(THF)_2$ can be reduced in toluene to give an insoluble product.

We have developed two procedures to make these compounds. The first involves the use of $M_2X_6(THT)_3$ as starting material. When this is dissolved in THF, $M_2X_6(\mu\text{-THT})(THF)_2$, the precursor to these compounds, forms. Reaction with sodium amalgam then produces the desired product. The second and superior procedure is a "two-step, one-pot" synthesis in which the commercially available pentahalides are used as starting materials. In the first step MX_5 is reduced in toluene to $M_2X_6(THT)_3$.

(16) (a) Leutkens, M. L., Jr.; Elcesser, W. L.; Huffman, J. C.; Sattelberger, A. P. *Inorg. Chem.* **1984**, *23*, 1718. (b) Datta, S.; Wreford, S. S. *Inorg. Chem.* **1977**, *16*, 1134.

(17) Coffindaffer, T. W.; Rothwell, I. P.; Folting, K.; Huffman, J. C.; Streib, W. E. *J. Chem. Soc., Chem. Commun.* **1985**, *1519*.

(18) Curtis, M. D.; Real, J. *Organometallics* **1985**, *4*, 940.

(19) Cotton, F. A.; Duraj, S. A.; Roth, W. J. *Acta Crystallogr., Sect. C: Cryst. Struct. Commun.* **1985**, *C41*, 878.

Table II. Positional and Isotropic-Equivalent Displacement Parameters for $(NEt_4)_2[Nb_2Cl_6(\mu\text{-}THT)_3]\cdot CH_3CN$ (**1c**)[a]

atom	x	y	z	B, Å²
Nb(1)	0.62662 (4)	0.29461 (3)	0.55118 (5)	2.69 (1)
Nb(2)	0.39421 (4)	0.22004 (3)	0.54679 (5)	2.80 (1)
Cl(1)	0.8065 (2)	0.35065 (9)	0.7522 (2)	4.60 (4)
Cl(2)	0.7614 (1)	0.23989 (9)	0.4501 (2)	4.41 (4)
Cl(3)	0.6946 (2)	0.41258 (8)	0.4545 (2)	4.53 (4)
Cl(4)	0.3116 (2)	0.18800 (9)	0.7407 (2)	5.01 (4)
Cl(5)	0.2796 (2)	0.08785 (9)	0.4401 (2)	5.04 (4)
Cl(6)	0.2086 (1)	0.26010 (9)	0.4500 (2)	4.60 (4)
S(1)	0.4619 (1)	0.24682 (8)	0.3538 (1)	3.58 (3)
S(2)	0.5701 (1)	0.18084 (7)	0.6436 (1)	3.08 (3)
S(3)	0.4991 (1)	0.34575 (7)	0.6542 (1)	3.01 (3)
C(1)	0.4079 (7)	0.3067 (4)	0.2422 (7)	5.9 (2)
C(2)	0.426 (1)	0.2803 (7)	0.1163 (9)	11.6 (4)
C(3)	0.408 (1)	0.2024 (8)	0.1025 (9)	11.6 (4)
C(4)	0.4616 (7)	0.1783 (5)	0.2286 (7)	5.9 (2)
C(5)	0.6251 (8)	0.1766 (4)	0.8145 (6)	5.3 (2)
C(6)	0.680 (1)	0.1141 (5)	0.8215 (9)	10.3 (3)
C(7)	0.696 (1)	0.0885 (5)	0.706 (1)	11.3 (3)
C(8)	0.5990 (6)	0.0969 (3)	0.5919 (7)	4.5 (2)
C(9)	0.5249 (6)	0.3684 (4)	0.8279 (6)	4.6 (2)
C(10)	0.4714 (9)	0.4287 (5)	0.8447 (9)	9.1 (3)
C(11)	0.4102 (9)	0.4483 (5)	0.7324 (9)	8.9 (2)
C(12)	0.4444 (6)	0.4235 (3)	0.6146 (7)	4.6 (2)
N(1)	0.9787 (5)	0.4055 (3)	0.2333 (5)	3.8 (1)*
C(13)	1.0771 (8)	0.3806 (5)	0.2036 (9)	6.9 (2)*
C(14)	1.206 (1)	0.4449 (6)	0.228 (1)	8.5 (3)*
C(15)	1.0176 (8)	0.4492 (4)	0.3695 (8)	5.9 (2)*
C(16)	1.0599 (7)	0.4028 (4)	0.4736 (8)	5.6 (2)*
C(17)	0.9472 (8)	0.4590 (5)	0.1392 (9)	6.9 (2)*
C(18)	0.8331 (9)	0.4810 (6)	0.149 (1)	8.1 (2)*
C(19)	0.8648 (8)	0.3387 (5)	0.2289 (8)	6.4 (2)*
C(20)	0.8040 (9)	0.2937 (6)	0.094 (1)	8.1 (2)*
N(2)	0.8745 (6)	0.0544 (3)	0.2464 (6)	5.3 (1)*
C(21)	0.757 (1)	0.0776 (8)	0.228 (2)	8.8 (4)*
C(21A)	0.744 (4)	0.009 (2)	0.190 (4)	10 (1)*
C(22)	0.649 (2)	0.019 (1)	0.261 (2)	12.6 (6)*
C(22A)	0.637 (5)	0.053 (3)	0.174 (5)	13 (2)*
C(23)	0.920 (1)	0.0398 (8)	0.381 (1)	7.7 (3)*
C(23A)	0.918 (4)	0.118 (2)	0.355 (4)	10 (1)*
C(24)	0.947 (1)	0.1069 (8)	0.487 (1)	7.9 (3)*
C(24A)	0.896 (3)	0.089 (2)	0.487 (3)	6.1 (6)*
C(25)	0.973 (2)	0.121 (1)	0.224 (2)	10.1 (5)*
C(25A)	0.913 (4)	0.108 (2)	0.148 (4)	10 (1)*
C(26)	1.062 (2)	0.119 (1)	0.162 (2)	11.1 (5)*
C(26A)	0.992 (3)	0.145 (2)	0.118 (3)	7.2 (7)*
C(27)	0.851 (1)	−0.0138 (7)	0.155 (1)	7.3 (3)*
C(27A)	0.940 (3)	−0.008 (2)	0.297 (3)	7.1 (7)*
C(28)	0.958 (2)	−0.0472 (9)	0.170 (2)	9.3 (4)*
C(28A)	0.778 (3)	−0.016 (2)	0.015 (3)	8.2 (8)*
N(3)	0.945 (1)	0.7262 (6)	0.277 (1)	11.0 (3)*
C(29)	0.926 (2)	0.7261 (9)	0.148 (2)	14.0 (5)*
C(30)	0.938 (2)	0.744 (1)	0.048 (3)	23 (1)*

[a] Atoms with an asterisk were refined isotropically. Anisotropically refined atoms are given in the form of the isotropic equivalent thermal parameter defined as $^4/_3[a^2\beta_{11} + b^2\beta_{22} + c^2\beta_{33} + ab(\cos\gamma)\beta_{12} + ac(\cos\beta)\beta_{13} + bc(\cos\alpha)\beta_{23}]$.

Although excess reducing agent is present, the reaction terminates with the formation of the M(III) complex. THF is then added, and the second step, reduction of $M_2X_6(\mu\text{-}THT)(THF)_2$ to $[M_2X_6(\mu\text{-}THT)_3]^{2-}$, takes place. Enough THF is added to produce a soluble ionic product. Addition of THF prior to the formation of $M_2X_6(THT)_3$ has been shown to result in the formation of M(IV) complexes only.[1a] This second method of preparation is similar to the first except that $M_2X_6(THT)_3$ is an intermediate rather than the starting material. The time consuming isolation of $M_2X_6(THT)_3$ is thereby avoided, and the overall yields based on the amount of MX_5 used are higher.

We felt that the above preparative procedures required further modification since the sodium salts tended to form insoluble oligomers, contaminated with NaCl, and the use of Li^+ did not guarantee complete exclusion of sodium cations or a product free of LiCl contamination. It was found that addition of 50–60% of the theoretically required amount of NEt_4Cl to the post reaction

Table III. Positional and Isotropic-Equivalent Displacement Parameters for $[Na(THF)_3]_2[Nb_2Cl_5(THT)_3]_2$ (**3**)[a]

atom	x	y	z	B, Å²
Nb(1)	0.2149 (2)	0.0678 (1)	0.3460 (1)	3.38 (4)
Nb(2)	0.3598 (1)	0.0152 (1)	0.4687 (1)	2.92 (4)
Cl(1)	0.1988 (4)	0.1936 (3)	0.2968 (5)	5.1 (2)
Cl(2)	0.1600 (5)	0.0345 (4)	0.1729 (4)	5.5 (2)
Cl(3)	0.0348 (4)	0.0669 (4)	0.3657 (4)	4.9 (2)
Cl(4)	0.3372 (4)	−0.0452 (3)	0.6196 (4)	4.9 (2)
Cl(5)	0.5131 (4)	0.0782 (3)	0.5587 (4)	3.7 (1)
S(1)	0.3865 (4)	0.0697 (3)	0.3197 (4)	3.8 (1)
S(2)	0.2543 (4)	0.1067 (3)	0.5122 (4)	4.0 (2)
S(3)	0.2252 (4)	−0.0544 (3)	0.3869 (4)	3.9 (1)
Na	0.0104 (6)	0.1437 (5)	0.1961 (6)	5.3 (3)
O(4)	−0.145 (1)	0.091 (1)	0.136 (1)	9.7 (6)
O(5)	−0.058 (1)	0.2481 (9)	0.265 (1)	6.1 (5)
O(6)	0.022 (1)	0.189 (1)	0.042 (1)	7.4 (5)
C(11)	0.425 (2)	0.024 (1)	0.215 (2)	4.2 (5)*
C(12)	0.442 (2)	0.085 (1)	0.149 (2)	7.3 (8)*
C(13)	0.481 (2)	0.147 (2)	0.203 (2)	8.0 (8)*
C(14)	0.454 (2)	0.150 (1)	0.306 (2)	5.0 (6)*
C(21)	0.296 (2)	0.197 (1)	0.549 (2)	5.6 (6)*
C(22)	0.220 (2)	0.218 (2)	0.612 (2)	8.6 (8)*
C(23)	0.193 (2)	0.156 (2)	0.665 (2)	8.8 (9)*
C(24)	0.169 (2)	0.095 (1)	0.600 (2)	4.9 (6)*
C(31)	0.131 (2)	−0.098 (1)	0.445 (1)	4.1 (5)*
C(32)	0.107 (3)	−0.160 (2)	0.386 (3)	12 (1)*
C(33)	0.146 (2)	−0.171 (2)	0.306 (2)	9.7 (9)*
C(34)	0.238 (2)	−0.124 (1)	0.297 (2)	5.3 (6)*
C(41)	−0.170 (4)	0.033 (3)	0.182 (4)	20 (2)*
C(42)	−0.264 (3)	0.004 (2)	0.129 (3)	14 (1)*
C(43)	−0.288 (3)	0.047 (2)	0.043 (3)	13 (1)*
C(44)	−0.193 (4)	0.089 (3)	0.045 (3)	17 (2)*
C(51)	−0.008 (2)	0.314 (1)	0.272 (2)	6.4 (7)*
C(52)	0.015 (3)	0.336 (2)	0.377 (3)	13 (1)*
C(53)	−0.050 (3)	0.289 (2)	0.423 (3)	14 (1)*
C(54)	−0.100 (2)	0.234 (2)	0.353 (2)	8.0 (8)*
C(61)	0.096 (2)	0.241 (2)	0.040 (2)	10 (1)*
C(62)	0.156 (3)	0.216 (2)	−0.036 (3)	15 (1)*
C(63)	0.099 (3)	0.171 (2)	−0.084 (3)	17 (2)*
C(64)	0.009 (3)	0.145 (2)	−0.045 (3)	16 (1)*

[a] Atoms with an asterisk were refined isotropically. Anisotropically refined atoms are given in the form of the isotropic equivalent thermal parameter defined as $^4/_3[a^2\beta_{11} + b^2\beta_{22} + c^2\beta_{33} + ab(\cos\gamma)\beta_{12} + ac(\cos\beta)\beta_{13} + bc(\cos\alpha)\beta_{23}]$.

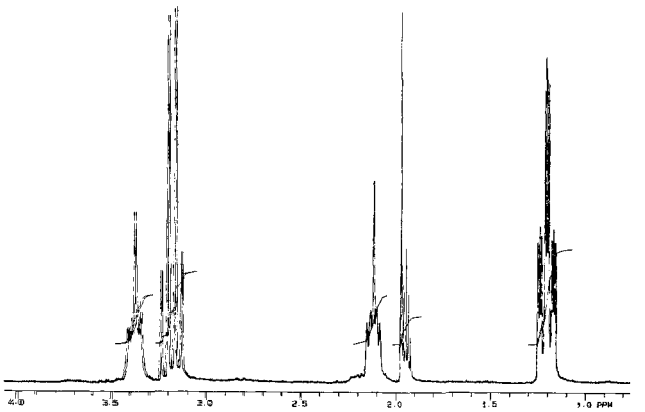

Figure 5. NMR spectrum of $[NEt_4]_2[Nb_2Cl_6(\mu\text{-}THT)_3]\cdot CH_3CN$ (**1c**) in CD_3CN.

solution afforded pure $[NEt_4]_2[Nb_2Cl_6(\mu\text{-}THT)_3]\cdot CH_3CN$ in about 45% overall yield when starting with $NbCl_5$. The use of larger quantities of NEt_4Cl gave a product contaminated with this salt, and purification by fractional crystallization was tedious and detrimental to the yield.

Proton NMR spectra confirm the diamagnetism of the dimers and the equivalence of the bridging THT ligands (see Figure 5). The apparent triplet and quintet are characteristic[2] of the protons bound to α and β-carbon atoms, respectively, in tetrahydrothiophene.

Unlike most known M(II) complexes (M = Nb, Ta), which

Table IV. Positional and Isotropic-Equivalent Displacement Parameters for $[Na(THF)_3]_2[Nb_2Br_5(THT)_3]_2$ (**4**)[a]

atom	x	y	z	B, Å²
Nb(1)	0.3140 (1)	0.20264 (9)	0.0726 (1)	3.14 (3)
Nb(2)	0.0980 (1)	0.10139 (9)	−0.0185 (1)	2.74 (3)
Br(1)	0.5136 (1)	0.1465 (1)	0.0693 (2)	5.16 (5)
Br(2)	0.4515 (2)	0.3138 (1)	0.3275 (2)	5.52 (5)
Br(3)	0.3693 (2)	0.3324 (1)	−0.0162 (2)	5.41 (5)
Br(4)	−0.1004 (1)	0.1112 (1)	−0.2181 (1)	4.41 (4)
Br(5)	−0.0327 (1)	0.0807 (1)	0.1275 (1)	3.58 (4)
S(1)	0.2767 (3)	0.0872 (3)	0.1625 (3)	3.12 (9)
S(2)	0.2031 (3)	0.1054 (3)	−0.1620 (3)	3.5 (1)
S(3)	0.1397 (3)	0.2605 (3)	0.0830 (4)	3.8 (1)
Na	0.6223 (6)	0.3375 (5)	0.1852 (7)	6.2 (2)
O(4)	0.679 (1)	0.4908 (9)	0.283 (2)	10.4 (6)
O(5)	0.712 (1)	0.3399 (9)	0.027 (1)	9.9 (5)
O(6)	0.799 (1)	0.329 (1)	0.371 (1)	9.8 (5)
C(11)	0.307 (1)	0.113 (1)	0.343 (1)	4.5 (4)
C(12)	0.410 (2)	0.069 (1)	0.397 (2)	7.4 (6)
C(13)	0.441 (2)	0.014 (1)	0.306 (2)	10.2 (8)
C(14)	0.352 (1)	−0.005 (1)	0.154 (1)	4.6 (4)
C(21)	0.147 (1)	0.145 (1)	−0.309 (1)	4.9 (4)
C(22)	0.188 (2)	0.093 (2)	−0.405 (2)	11.9 (8)
C(23)	0.220 (2)	0.010 (2)	−0.386 (2)	11.2 (8)
C(24)	0.258 (1)	0.010 (1)	−0.239 (1)	5.6 (5)
C(31)	0.129 (1)	0.319 (1)	0.243 (1)	5.0 (5)
C(32)	0.069 (2)	0.391 (2)	0.218 (2)	14.1 (9)
C(33)	0.069 (2)	0.414 (1)	0.110 (2)	9.0 (8)
C(34)	0.074 (1)	0.336 (1)	−0.005 (2)	5.6 (5)
C(41)	0.594 (2)	0.536 (1)	0.300 (3)	13 (1)
C(42)	0.654 (2)	0.632 (2)	0.364 (2)	10.9 (9)
C(43)	0.786 (3)	0.635 (1)	0.386 (2)	13 (1)
C(44)	0.794 (2)	0.544 (2)	0.320 (3)	14 (1)
C(51)	0.704 (2)	0.255 (2)	−0.071 (2)	12.5 (8)
C(52)	0.646 (3)	0.263 (2)	−0.212 (3)	14 (1)
C(53)	0.686 (2)	0.363 (2)	−0.170 (3)	12 (1)
C(54)	0.692 (2)	0.404 (2)	−0.036 (2)	12.2 (9)
C(61)	0.837 (2)	0.251 (2)	0.367 (3)	13 (1)
C(62)	0.844 (4)	0.238 (2)	0.479 (3)	20 (2)
C(63)	0.844 (3)	0.315 (2)	0.572 (2)	20 (1)
C(64)	0.820 (3)	0.369 (2)	0.504 (2)	15 (1)

[a] Atoms with an asterisk were refined isotropically. Anisotropically refined atoms are given in the form of the isotropic equivalent thermal parameter defined as $^4/_3[a^2\beta_{11} + b^2\beta_{22} + c^2\beta_{33} + ab(\cos\gamma)\beta_{12} + ac(\cos\beta)\beta_{13} + bc(\cos\alpha)\beta_{23}]$.

Table V. Positional and Isotropic-Equivalent Displacement Parameters for $[Li(THF)_2]_2[Ta_2Cl_6(THT)_3]$ (**5a**)[a]

atom	x	y	z	B, Å²
Ta(1)	0.2094 (1)	0.30423 (5)	0.0984 (1)	3.83 (3)
Ta(2)	0.1381 (1)	0.18899 (5)	−0.03917 (9)	3.55 (2)
Cl(1)	0.0669 (8)	0.3954 (3)	0.0069 (7)	5.8 (2)
Cl(2)	0.2361 (8)	0.3540 (4)	0.3511 (6)	6.0 (2)
Cl(3)	0.4348 (7)	0.3592 (4)	0.1622 (7)	6.4 (2)
Cl(4)	0.0939 (7)	0.1043 (3)	0.0577 (7)	6.1 (2)
Cl(5)	0.2888 (7)	0.1153 (4)	−0.1202 (7)	5.7 (2)
Cl(6)	−0.0821 (7)	0.1507 (3)	−0.2805 (7)	6.0 (2)
S(1)	−0.0099 (6)	0.2552 (3)	0.0382 (6)	4.3 (2)
S(2)	0.1803 (7)	0.2631 (3)	−0.1448 (6)	4.4 (2)
S(3)	0.3495 (7)	0.2212 (3)	0.1985 (6)	4.8 (2)
C(11)	−0.059 (3)	0.244 (2)	0.181 (3)	7.9 (9)*
C(12)	−0.222 (6)	0.265 (3)	0.115 (5)	16 (2)*
C(13)	−0.286 (6)	0.255 (3)	−0.041 (6)	18 (2)*
C(14)	−0.194 (3)	0.277 (2)	−0.095 (3)	7.4 (8)*
C(21)	0.326 (3)	0.261 (1)	−0.191 (3)	6.6 (7)*
C(22)	0.279 (4)	0.294 (2)	−0.310 (4)	12 (1)*
C(23)	0.132 (3)	0.297 (2)	−0.388 (3)	7.3 (8)*
C(24)	0.040 (3)	0.289 (1)	−0.314 (3)	6.0 (7)*
C(31)	0.376 (3)	0.202 (1)	0.372 (3)	6.3 (7)*
C(32)	0.538 (4)	0.197 (2)	0.460 (4)	10 (1)*
C(33)	0.624 (4)	0.197 (2)	0.393 (4)	10 (1)*
C(34)	0.542 (3)	0.211 (1)	0.238 (3)	6.8 (7)*
O(4)	0.258 (3)	0.518 (2)	0.331 (3)	15 (1)*
C(41)	0.343 (4)	0.516 (2)	0.256 (4)	12 (1)*
C(42)	0.393 (5)	0.583 (2)	0.295 (5)	14 (2)*
C(43)	0.341 (4)	0.614 (2)	0.399 (4)	12 (1)*
C(44)	0.267 (5)	0.580 (3)	0.433 (5)	15 (2)*
O(5)	−0.043 (5)	0.473 (2)	0.282 (4)	22 (2)*
C(51)	−0.165 (7)	0.504 (3)	0.162 (7)	22 (3)*
C(52)	−0.315 (8)	0.511 (4)	0.091 (8)	26 (3)*
C(53)	−0.269 (7)	0.492 (3)	0.249 (7)	22 (3)*
C(54)	−0.16 (1)	0.434 (5)	0.28 (1)	35 (5)*
O(6)	0.335 (2)	−0.014 (1)	0.043 (2)	8.5 (6)*
C(61)	0.460 (4)	0.020 (2)	0.174 (4)	9 (1)*
C(62)	0.477 (5)	−0.004 (3)	0.303 (5)	15 (2)*
C(63)	0.400 (4)	−0.066 (2)	0.239 (4)	12 (1)*
C(64)	0.306 (4)	−0.072 (2)	0.077 (4)	11 (1)*
O(7)	0.055 (2)	−0.021 (1)	−0.267 (2)	8.6 (6)*
C(71)	0.112 (5)	−0.076 (2)	−0.338 (5)	13 (2)*
C(72)	−0.027 (4)	−0.114 (2)	−0.426 (4)	11 (1)*
C(73)	−0.149 (4)	−0.076 (2)	−0.449 (4)	10 (1)*
C(74)	−0.094 (4)	−0.019 (2)	−0.329 (4)	9 (1)*
Li(1)	0.14 (1)	0.445 (5)	0.26 (1)	15 (3)*
Li(2)	0.178 (7)	0.032 (3)	−0.085 (6)	9 (2)*

[a] Atoms with an asterisk were refined isotropically. Anisotropically refined atoms are given in the form of the isotropic equivalent thermal parameter defined as $^4/_3[a^2\beta_{11} + b^2\beta_{22} + c^2\beta_{33} + ab(\cos\gamma)\beta_{12} + ac(\cos\beta)\beta_{13} + bc(\cos\alpha)\beta_{23}]$.

are very reactive, the $M_2X_6(\mu\text{-THT})_3^{2-}$ compounds are fairly inert. They react with carboxylic acids by oxidation to the +4 oxidation state, and they dissociate in pyridine to give $MCl_2(py)_4$, but otherwise they seem unreactive toward most other donor ligands and can even be recrystallized unchanged from degassed water. This high stability can probably be attributed to several factors, including (1) that these compounds are 18-electron species, (2) that they are d^3 metals in octahedral environments, which usually leads to kinetic stability, and 3) that in solutions of the alkali salts the solvated counterions probably bind to the ends of these molecules as they do in the solid state. This would tend to protect the molecules from incoming reactants.

Electronic Structure and Metal–Metal Bonding. The interpretation of bonding in face sharing bioctahedral complexes is complicated by the presence of three bridging atoms. Simple correlations do not exist between the number of valence d electrons present and either the M–M distance or the M–M bond order.[8] Since these are the first and only examples of discrete Nb or Ta complexes containing metal–metal triple bonds, a direct comparison to analogous compounds is not possible. However, several structurally similar group 5 complexes containing M–M double bonds are known.[19] The metal–metal distances exhibited by the triply bonded compounds fall in the narrow range of 2.607–2.632 Å while the distances in the double-bonded complexes in which the three bridging atoms are third-row main-group elements are between 2.67 and 2.71 Å. This shortening of the M–M distance by nearly 0.1 Å can be explained readily by the occupation of a third metal–metal bonding molecular orbital by the additional pair of electrons.

The nature of the metal–metal molecular orbitals in a face-sharing bioctahedron has been discussed before.[20] Qualitatively the type of M–M bonding involved is most easily developed conceptually by using the atomic d orbitals of two metal atoms in unperturbed octahedral environments as a starting point. The four atomic orbitals of local e_g symmetry combine to form molecular e′ and e″ orbitals (for molecular symmetry D_{3h}), as shown in Figure 6A. These orbitals can be thought of as hybrids of conventional M–M π and M–M δ orbitals with about twice as much π character as δ character. The e′ orbital is M–M bonding, and the e″ orbital is M–M antibonding, but because both orbitals are strongly M–L σ antibonding (since they are developed from the local e_g set), they are of high energy. The six orbitals of atomic t_{2g} symmetry combine to form molecular a_1', e′, e″, and a_2' orbitals. The a_1' and a_2' orbitals are of M–M σ and M–M σ^* symmetry, respectively. The two sets of degenerate orbitals are again hybrids of π- and δ-type orbitals, but this time with about twice as much δ character as π. In our case there are six valence d electrons

(20) (a) Cotton, F. A.; Ucko, D. A. *Inorg. Chim. Acta* **1972**, *6*, 161. (b) Bursten, B. E.; Cotton, F. A.; Fang, A. *Inorg. Chem.* **1983**, *22*, 2127. (c) Templeton, J. L.; Dorman, W. C.; Clardy, J. C.; McCarley, R. E. *Inorg. Chem.* **1978**, *17*, 1263. (d) Sommerville, R. H.; Hoffman, R. *J. Am. Chem. Soc.* **1979**, *101*, 3821.

Table VI. Positional and Isotropic-Equivalent Displacement Parameters for $Na_2[Ta_2Cl_6(THT)_3]\cdot{}^3/_2THF$ (**5b**)[a]

atom	x	y	z	B, Å²
Ta(1)	0.21304 (3)	0.24910 (2)	0.22119 (2)	2.525 (6)
Ta(2)	0.14660 (3)	0.12569 (2)	0.14643 (2)	2.376 (6)
Cl(11)	0.1420 (2)	0.3710 (1)	0.1631 (2)	4.20 (5)
Cl(12)	0.4329 (2)	0.2977 (1)	0.2666 (2)	4.26 (5)
Cl(13)	0.1823 (2)	0.2887 (1)	0.3639 (1)	4.24 (5)
Cl(21)	−0.0100 (2)	0.1035 (1)	−0.0007 (1)	3.40 (4)
Cl(22)	0.2871 (2)	0.0319 (1)	0.1052 (2)	3.74 (5)
Cl(23)	0.0442 (2)	0.0240 (1)	0.2060 (1)	3.71 (5)
S(1)	0.2462 (2)	0.2168 (1)	0.0832 (1)	2.78 (4)
S(2)	−0.0015 (2)	0.2082 (1)	0.1774 (1)	2.85 (4)
S(3)	0.2930 (2)	0.1373 (1)	0.2860 (1)	3.28 (5)
Na(1)	0.1371 (4)	0.0074 (3)	−0.0579 (2)	4.71 (9)
Na(2)	0.3091 (4)	0.4094 (2)	0.3252 (3)	4.65 (9)
O(4)	0.2694 (9)	0.0388 (9)	−0.1381 (6)	12.7 (4)
C(11)	0.4033 (9)	0.2074 (7)	0.0625 (7)	4.7 (2)
C(12)	0.392 (1)	0.249 (1)	−0.0183 (9)	10.7 (5)
C(13)	0.270 (1)	0.261 (1)	−0.0695 (8)	12.1 (5)
C(14)	0.175 (1)	0.2642 (6)	−0.0193 (6)	4.4 (2)
C(21)	−0.1301 (9)	0.2496 (6)	0.0921 (7)	4.3 (2)
C(22)	−0.248 (1)	0.225 (1)	0.113 (1)	10.6 (6)
C(23)	−0.235 (1)	0.195 (1)	0.1953 (9)	10.1 (6)
C(24)	−0.102 (1)	0.1883 (7)	0.2501 (6)	5.0 (3)
C(31)	0.268 (1)	0.1015 (6)	0.3866 (6)	5.2 (3)
C(32)	0.405 (1)	0.0888 (9)	0.4440 (7)	8.0 (4)
C(33)	0.487 (1)	0.0638 (8)	0.3900 (9)	6.9 (4)
C(34)	0.463 (1)	0.1115 (6)	0.3115 (8)	5.1 (3)
C(41)	0.399 (1)	0.035 (1)	−0.118 (1)	11.5 (6)
C(42)	0.421 (2)	0.063 (1)	−0.202 (1)	14.3 (7)
C(43)	0.322 (2)	0.070 (2)	−0.261 (1)	18 (1)
C(44)	0.219 (2)	0.063 (2)	−0.225 (1)	20 (1)
O(5)	0.626 (5)	0.530 (3)	0.019 (4)	16 (2)*
C(51)	0.578 (5)	0.519 (3)	0.044 (3)	19 (2)*
C(52)	0.507 (5)	0.459 (3)	0.050 (3)	22 (2)*

[a] Atoms with an asterisk were refined isotropically. Anisotropically refined atoms are given in the form of the isotropic equivalent thermal parameter defined as $^4/_3[a^2\beta_{11} + b^2\beta_{22} + c^2\beta_{33} + ab(\cos\gamma)\beta_{12} + ac(\cos\beta)\beta_{13} + bc(\cos\alpha)\beta_{23}]$.

Table VII. Important Bond Distances (Å) and Angles (deg) for $(NEt_4)_2[Nb_2Cl_6(THT)_3]\cdot CH_3CN$ (**1c**)[a]

Bond Distances			
Nb(1)–Nb(2)	2.632 (1)	Nb(2)–Cl(4)	2.537 (1)
Nb(1)–Cl(1)	2.558 (1)	Nb(2)–Cl(5)	2.544 (1)
Nb(1)–Cl(2)	2.536 (1)	Nb(2)–Cl(6)	2.529 (1)
Nb(1)–Cl(3)	2.535 (1)	Nb(2)–S(1)	2.429 (1)
Nb(1)–S(1)	2.430 (1)	Nb(2)–S(2)	2.424 (1)
Nb(1)–S(2)	2.428 (1)	Nb(2)–S(3)	2.434 (1)
Nb(1)–S(3)	2.438 (1)		
Bond Angles			
Cl(1)–Nb(1)–Cl(2)	91.45 (5)	Cl(4)–Nb(2)–S(1)	176.85 (5)
Cl(1)–Nb(1)–Cl(3)	89.95 (5)	Cl(4)–Nb(2)–S(2)	87.79 (4)
Cl(1)–Nb(1)–S(1)	176.71 (4)	Cl(4)–Nb(2)–S(3)	88.62 (4)
Cl(1)–Nb(1)–S(2)	88.97 (4)	Cl(5)–Nb(2)–Cl(6)	92.02 (5)
Cl(1)–Nb(1)–S(3)	87.41 (4)	Cl(5)–Nb(2)–S(1)	88.28 (5)
Cl(2)–Nb(1)–Cl(3)	91.51 (4)	Cl(5)–Nb(2)–S(2)	87.91 (4)
Cl(2)–Nb(1)–S(1)	87.65 (4)	Cl(5)–Nb(2)–S(3)	177.93 (5)
Cl(2)–Nb(1)–S(2)	86.27 (4)	Cl(6)–Nb(2)–S(1)	87.06 (5)
Cl(2)–Nb(1)–S(3)	178.29 (4)	Cl(6)–Nb(2)–S(2)	178.68 (5)
Cl(3)–Nb(1)–S(1)	86.92 (4)	Cl(6)–Nb(2)–S(3)	87.40 (4)
Cl(3)–Nb(1)–S(2)	177.51 (4)	S(1)–Nb(2)–S(2)	94.25 (4)
Cl(3)–Nb(1)–S(3)	89.76 (4)	S(1)–Nb(2)–S(3)	93.68 (4)
S(1)–Nb(1)–S(2)	94.12 (4)	S(2)–Nb(2)–S(3)	92.63 (4)
S(1)–Nb(1)–S(3)	93.56 (4)	Nb(1)–S(1)–Nb(2)	65.60 (3)
S(2)–Nb(1)–S(3)	92.43 (4)	Nb(1)–S(2)–Nb(2)	65.71 (3)
Cl(4)–Nb(2)–Cl(5)	89.40 (5)	Nb(1)–S(3)–Nb(2)	65.41 (3)
Cl(4)–Nb(2)–Cl(6)	90.90 (5)		

[a] Numbers in parentheses are estimated standard deviations in the least significant digits.

available for metal–metal bonding, and they fill the a_1' and e' (t_{2g}) orbitals to give a net M–M bond order of 3.

A more quantitative description of the metal–metal bonding can be gained from molecular orbital calculations. A Fenske–Hall type MO calculation[21] was made on the model compound $Nb_2Cl_6(\mu\text{-}SH_2)_3^{2-}$, idealized to D_{3h} symmetry, and the energy level diagram obtained is presented in Figure 6B. This calculation confirms the basic ordering and composition of the valence molecular orbitals described above and supports our assignment of a M–M triple bond.

Table VIII. Important Bond Distances (Å) and Angles (deg) for $[Na(THF)_3]_2[Nb_2X_5(THT)_3]_2$, X = Cl (**3**) and Br (**4**)[a]

	3	4
Bond Distances		
Nb(1)–Nb(2)	2.610 (3)	2.607 (2)
Nb(1)–X(1)	2.520 (6)	2.682 (2)
Nb(1)–X(2)	2.517 (6)	2.683 (2)
Nb(1)–X(3)	2.518 (6)	2.683 (2)
Nb(1)–S(1)	2.432 (5)	2.429 (4)
Nb(1)–S(2)	2.436 (6)	2.421 (4)
Nb(1)–S(3)	2.422 (6)	2.427 (4)
Nb(2)–Nb(2)′	3.827 (4)	4.061 (3)
Nb(2)–X(4)	2.489 (6)	2.658 (2)
Nb(2)–X(5)	2.566 (5)	2.748 (2)
Nb(2)–X(5)′	2.571 (5)	2.741 (2)
Nb(2)–S(1)	2.432 (6)	2.436 (4)
Nb(2)–S(2)	2.419 (6)	2.420 (4)
Nb(2)–S(3)	2.409 (6)	2.412 (5)
Bond Angles		
X(1)–Nb(1)–X(2)	88.8 (2)	86.6 (1)
X(1)–Nb(1)–X(3)	89.7 (2)	89.7 (1)
X(1)–Nb(1)–S(1)	89.2 (2)	87.8 (1)
X(1)–Nb(1)–S(2)	88.0 (2)	88.0 (1)
X(1)–Nb(1)–S(3)	177.5 (2)	177.2 (1)
X(2)–Nb(1)–X(3)	88.0 (2)	87.9 (1)
X(2)–Nb(1)–S(1)	89.7 (2)	89.7 (1)
X(2)–Nb(1)–S(2)	174.7 (2)	175.4 (1)
X(1)–Nb(1)–S(3)	88.9 (2)	89.0 (1)
X(3)–Nb(1)–S(1)	177.5 (2)	176.6 (1)
X(3)–Nb(1)–S(2)	87.7 (2)	89.1 (1)
X(3)–Nb(1)–S(3)	89.2 (2)	88.8 (1)
S(1)–Nb(1)–S(2)	94.4 (2)	93.2 (1)
S(1)–Nb(1)–S(3)	91.8 (2)	93.6 (1)
S(2)–Nb(1)–S(3)	94.3 (2)	94.4 (1)
X(4)–Nb(2)–X(5)	90.2 (2)	90.2 (1)
X(4)–Nb(2)–X(5)′	89.1 (2)	90.8 (1)
X(4)–Nb(2)–S(1)	177.4 (2)	178.1 (1)
X(4)–Nb(2)–S(2)	87.7 (2)	87.5 (1)
X(4)–Nb(2)–S(3)	87.6 (2)	88.0 (1)
X(5)–Nb(2)–X(5)′	83.7 (2)	84.7 (1)
X(5)–Nb(2)–S(1)	89.9 (2)	87.9 (1)
X(5)–Nb(2)–S(2)	90.1 (2)	90.2 (1)
X(5)–Nb(2)–S(3)	174.4 (2)	174.7 (1)
X(5)′–Nb(2)–S(1)	88.4 (2)	88.5 (1)
X(5)′–Nb(2)–S(2)	173.0 (2)	174.5 (1)
X(5)′–Nb(2)–S(3)	91.1 (2)	90.3 (1)
S(1)–Nb(2)–S(2)	94.9 (2)	93.1 (1)
S(1)–Nb(2)–S(3)	92.1 (2)	93.8 (1)
S(2)–Nb(2)–S(3)	95.0 (2)	94.8 (1)
Nb(2)–X(5)–Nb(2)′	96.3 (2)	95.3 (1)
Nb(1)–S(1)–Nb(2)	64.9 (1)	64.8 (1)
Nb(1)–S(2)–Nb(2)	65.0 (2)	65.2 (1)
Nb(1)–S(3)–Nb(2)	65.4 (2)	65.2 (1)

[a] Numbers in parentheses are estimated standard deviations in the least significant digits.

The bonding in the tetramers **3** and **4** is slightly more complicated. On the basis of the metal–metal distances a triple bond can be assigned between each of the outer pairs of metal atoms, while the inner pair interaction is nonbonding and in fact, based on the Nb–X(5)–Nb′ angles of 96.3° and 95.3°, repulsive. For a tetramer of this type, with a total of 12 electrons available for metal–metal bonding, the bonding sequence M≡M···M≡M, as found here, might well have been expected. For example, the sequence M=M=M=M leads to a mixed-valence species (M(III)–M(I)–M(I)–M(III)) and suffers because the inner two metal atoms both participate in four M–M bonds while there are only

(21) Hall, M. B.; Frenske, R. F. *Inorg. Chem.* **1972**, *11*, 768.

Table IX. Important Bond Distances (Å) and Angles (deg) for $[Li(THF)_2]_2[Ta_2Cl_6(THT)_3]$ (**5a**)[a]

	Bond Distances		
Ta(1)–Ta(2)	2.626 (1)	Ta(2)–Cl(4)	2.532 (6)
Ta(1)–Cl(1)	2.529 (6)	Ta(2)–Cl(5)	2.508 (7)
Ta(1)–Cl(2)	2.531 (6)	Ta(2)–Cl(6)	2.491 (5)
Ta(1)–Cl(3)	2.496 (6)	Ta(2)–S(1)	2.381 (6)
Ta(1)–S(1)	2.385 (6)	Ta(2)–S(2)	2.386 (6)
Ta(1)–S(2)	2.396 (6)	Ta(2)–S(3)	2.406 (5)
Ta(1)–S(3)	2.395 (6)		
	Bond Angles		
Cl(1)–Ta(1)–Cl(2)	87.5 (2)	Cl(4)–Ta(2)–S(1)	90.8 (2)
Cl(1)–Ta(1)–Cl(3)	89.2 (2)	Cl(4)–Ta(2)–S(2)	175.8 (2)
Cl(1)–Ta(1)–S(1)	88.9 (2)	Cl(4)–Ta(2)–S(3)	88.5 (2)
Cl(1)–Ta(1)–S(2)	89.2 (2)	Cl(5)–Ta(2)–Cl(6)	90.5 (2)
Cl(1)–Ta(1)–S(3)	176.9 (2)	Cl(5)–Ta(2)–S(1)	177.5 (2)
Cl(2)–Ta(1)–Cl(3)	90.5 (2)	Cl(5)–Ta(2)–S(2)	89.6 (2)
Cl(2)–Ta(1)–S(1)	88.6 (2)	Cl(5)–Ta(2)–S(3)	89.0 (2)
Cl(2)–Ta(1)–S(2)	176.5 (2)	Cl(6)–Ta(2)–S(1)	88.6 (2)
Cl(2)–Ta(1)–S(3)	89.5 (2)	Cl(6)–Ta(2)–S(2)	89.4 (2)
Cl(3)–Ta(1)–S(1)	177.9 (3)	Cl(6)–Ta(2)–S(3)	176.8 (2)
Cl(3)–Ta(1)–S(2)	88.4 (2)	S(1)–Ta(2)–S(2)	92.7 (2)
Cl(3)–Ta(1)–S(3)	89.9 (2)	S(1)–Ta(2)–S(3)	91.8 (2)
S(1)–Ta(1)–S(2)	92.4 (2)	S(2)–Ta(2)–S(3)	93.7 (2)
S(1)–Ta(1)–S(3)	92.0 (2)	Ta(1)–S(1)–Ta(2)	66.9 (2)
S(2)–Ta(1)–S(3)	93.8 (2)	Ta(1)–S(2)–Ta(2)	66.6 (2)
Cl(4)–Ta(2)–Cl(5)	86.8 (2)	Ta(1)–S(3)–Ta(2)	66.3 (1)
Cl(4)–Ta(2)–Cl(6)	88.3 (2)		

[a] Numbers in parentheses are estimated standard deviations in the least significant digits.

Table X. Important Bond Distances (Å) and Angles (deg) for $Na_2[Ta_2Cl_6(THT)_3]\cdot{}^3/_2THF$ (**5b**)[a]

	Bond Distances		
Ta(1)–Ta(2)	2.6156 (5)	Ta(2)–Cl(21)	2.556 (2)
Ta(1)–Cl(11)	2.510 (2)	Ta(2)–Cl(22)	2.544 (2)
Ta(1)–Cl(12)	2.511 (2)	Ta(2)–Cl(23)	2.526 (2)
Ta(1)–Cl(13)	2.507 (2)	Ta(2)–S(1)	2.394 (2)
Ta(1)–S(1)	2.408 (2)	Ta(2)–S(2)	2.395 (2)
Ta(1)–S(2)	2.409 (2)	Ta(2)–S(3)	2.392 (2)
Ta(1)–S(3)	2.398 (2)		
	Bond Angles		
Cl(11)–Ta(1)–Cl(12)	87.70 (9)	Cl(21)–Ta(2)–S(1)	90.06 (8)
Cl(11)–Ta(1)–Cl(13)	87.90 (9)	Cl(21)–Ta(2)–S(2)	87.94 (7)
Cl(11)–Ta(1)–S(1)	89.87 (8)	Cl(21)–Ta(2)–S(3)	175.82 (8)
Cl(11)–Ta(1)–S(2)	89.75 (8)	Cl(22)–Ta(2)–Cl(23)	86.66 (8)
Cl(11)–Ta(1)–S(3)	175.40 (8)	Cl(22)–Ta(2)–S(1)	90.14 (8)
Cl(12)–Ta(1)–Cl(13)	89.08 (9)	Cl(22)–Ta(2)–S(2)	174.84 (8)
Cl(12)–Ta(1)–S(1)	89.14 (8)	Cl(22)–Ta(2)–S(3)	89.88 (8)
Cl(12)–Ta(1)–S(2)	177.29 (8)	Cl(23)–Ta(2)–S(1)	176.29 (8)
Cl(12)–Ta(1)–S(3)	88.60 (8)	Cl(23)–Ta(2)–S(2)	90.56 (8)
Cl(13)–Ta(1)–S(1)	177.20 (8)	Cl(23)–Ta(2)–S(3)	88.58 (8)
Cl(13)–Ta(1)–S(2)	89.89 (8)	S(1)–Ta(2)–S(2)	92.48 (8)
Cl(13)–Ta(1)–S(3)	89.31 (9)	S(1)–Ta(2)–S(3)	93.29 (8)
S(1)–Ta(1)–S(2)	91.79 (7)	S(2)–Ta(2)–S(3)	94.40 (8)
S(1)–Ta(1)–S(3)	92.81 (8)	Ta(1)–S(1)–Ta(2)	65.99 (6)
S(2)–Ta(1)–S(3)	93.90 (8)	Ta(1)–S(2)–Ta(2)	65.98 (6)
Cl(21)–Ta(2)–Cl(22)	87.61 (8)	Ta(1)–S(3)–Ta(2)	66.19 (6)
Cl(21)–Ta(2)–Cl(23)	87.94 (8)		

[a] Numbers in parentheses are estimated standard deviations in least significant digits.

three atomic orbitals on each metal (the t_{2g} set) available for M–M bonding.

To assign the observed UV–visible absorption spectra, we must abandon the above simple molecular orbital description of M–M bonding. This is because the metal–metal interactions are weak enough that a MO description of the M–M bonding will overemphasize the ionic terms of the wave functions to the extent that accurate transition energies could not be predicted. The valence bond approach, in which the ionic terms are ignored rather than overemphasized, is a better approximation to use to assign the observed transitions than is the simple single configuration molecular orbital approach outlined above. Using valence bond

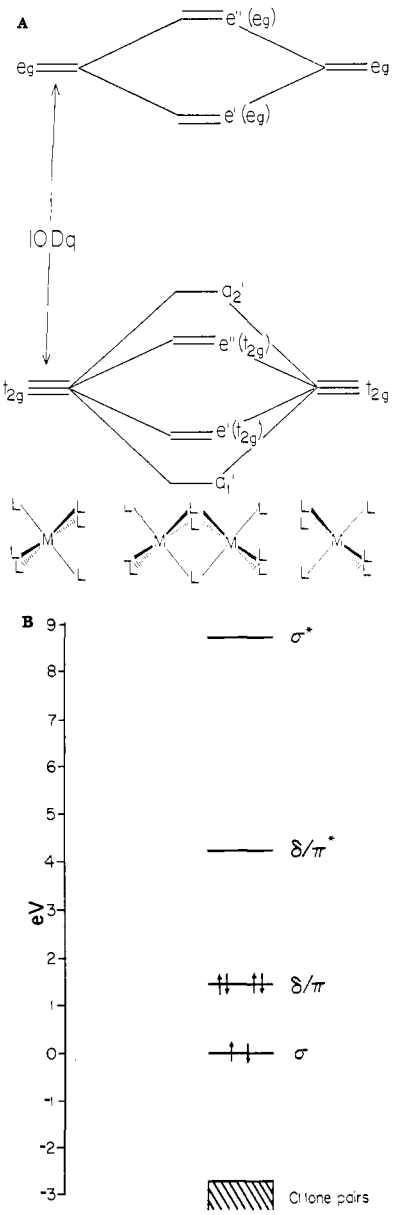

Figure 6. A. Qualitative molecular orbital diagram of the metal–metal bonding and antibonding orbitals in ideal face-sharing bioctahedra. B. Results of a Fenske–Hall calculation on $Nb_2Cl_6(SH_2)_3^{2-}$.

theory, Trogler was the first to assign successfully the absorption spectra for face-sharing bioctahedral compounds in which metal–metal bonding was important.[22] In the triply bonded complex $[W_2Cl_9]^{3-}$ three peaks in the visible spectrum were observed at 13 530, 17 200, and 25 600 cm^{-1}. The bands were assigned to the transitions $e'(t_{2g}) \rightarrow e'(e_g)$, $a_1' \rightarrow e'(e_g)$, and $a_1' \rightarrow a_2'$, respectively. We have observed only two peaks in the spectra of the $[M_2Cl_6(\mu\text{-THT})_3]^{2-}$ ions, one at 18 700 cm^{-1} and the other at 24 400 cm^{-1} (see Figure 7). For comparison, $10Dq$ in $NbCl_6^{4-}$ has been measured at 22 730 cm^{-1}.[23] We feel the most probable assignment of the observed bands would be to the $a_1' \rightarrow e'(e_g)$ and $a_1' \rightarrow a_2'$ transitions, respectively. The $e'(t_{2g}) \rightarrow e'(e_g)$ transition, which was lowest in intensity for $[W_2Cl_9]^{3-}$, would presumably be at lower energies, although we could not observe any other peaks with our spectrometer. However, we cannot rule out the alternative assignment of the two observed bands to the $e'(t_{2g}) \rightarrow e'(e_g)$ and $a_1' \rightarrow e'(e_g)$ transitions, with the $a_1' \rightarrow a_2'$ transition obscured by a charge-transfer band that dominates the spectra at higher energies. For $Nb_2Br_6(\mu\text{-THT})_3^{2-}$ only one peak (at 19 300 cm^{-1})

(22) Trogler, W. C. *Inorg. Chem.* **1980**, *19*, 697.
(23) Basu, S. *J. Inorg. Nucl. Chem.* **1966**, *28*, 2769.

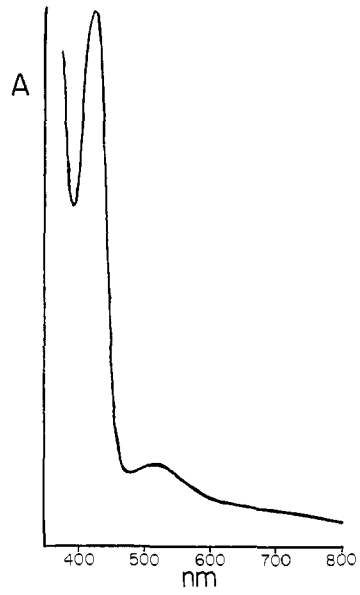

Figure 7. UV-vis spectrum of a dilute solution of $Na_2[Nb_2Cl_6(\mu\text{-}THT)_3]\cdot n$THF (**1b**) in THF.

energies. For $Nb_2Br_6(\mu\text{-}THT)_3^{2-}$ only one peak (at 19 300 cm^{-1}) was seen. The higher energy absorption seen in the chloride complexes was probably obscured in this case by a charge-transfer band which dominates the spectra at energies above 23 000 cm^{-1}.

In closing, we note a relevant recent development in this area. The compound $NaNb_3O_5F$ contains pairs of Nb(II) atoms at a distance of 2.61 Å from one another,[24] and this short distance led to the proposal of a triple Nb-Nb bond. The remainder of the coordination about each of the metal atoms is provided by a planar arrangement of four X atoms (X = O or F; these elements could not be distinguished crystallographically). The X atoms are eclipsed, and the Nb_2X_8 substructure is reminiscent of the class of structures typified by $Re_2Cl_8^{2-}$.[8] The metal-metal bonding picture is complicated by the presence of four Nb(IV) atoms at just over 3 Å away from the Nb(II) atoms. The extent to which these Nb(IV) atoms perturb the Nb(II)-Nb(II) triple bond and the exact nature of the bonding in this compound are uncertain. The experimental difficulties posed by this compound are such that these uncertainties will perhaps be resolved only through theoretical calculations.

Acknowledgment. We are grateful to the National Science Foundation and the Robert A. Welch Foundation for support of this work. M.P.D thanks the National Science Foundation for a NSF Predoctoral Fellowship and the Industry-University Cooperative Chemistry Program of Texas A&M for additional support.

Supplementary Material Available: Tables of anisotropic displacement parameters and complete listings of bond distances and bond angles for the crystal structures of **1c**, **3**, **4**, **5a**, and **5b** (22 pages); tables of observed and calculated structure factors for all five structures (85 pages). Ordering information is given on any current masthead page.

(24) Köhler, J.; Simon, A. *Angew. Chem., Int. Ed. Engl.* **1986**, *25*, 996.

Absolute Stereochemical Course of the 3-Carboxymuconate Cycloisomerases from *Pseudomonas putida* and *Acinetobacter calcoaceticus*: Analysis and Implications[1]

Ravi V. J. Chari,[†] Christian P. Whitman,[‡] John W. Kozarich,*[§] Ka-Leung Ngai,[⊥] and L. Nicholas Ornston[⊥]

Contribution from the Department of Chemistry and Biochemistry, University of Maryland, College Park, Maryland 20742, Department of Pharmacology, Yale University School of Medicine, New Haven, Connecticut 06510, and Department of Biology, Yale University, New Haven, Connecticut 06511. *Received February 23, 1987*

Abstract: The absolute stereochemical course of the 3-carboxymuconate cycloisomerases [EC 5.5.1.2; 2-carboxy-5-oxo-2,5-dihydrofuran-2-acetate lyase (decyclizing)] from *Pseudomonas putida* and *Acinetobacter calcoaceticus* has been determined by chemical and ^{1}H NMR methods. The product of the enzyme-catalyzed reaction in ^2H_2O was detected by NMR and trapped by catalytic hydrogenation to afford 5-[^{2}H]homocitrate lactone. Subsequent chemical degradation of the monodeuteriated homocitrate lactone gave (2*R*,3*S*)-2-[^{2}H]citrate as determined by ^{1}H NMR analysis. The product of the cycloisomerase reaction was established as (4*R*,5*R*)-5-[^{2}H]-4-carboxymuconate, indicating that the lactonization proceeded by an anti addition—the mechanistic and stereochemical antipode of the previously studied muconate cycloisomerase from *P. putida* and 3-carboxymuconate cycloisomerase from *Neurospora crassa*. The anti addition probably represents the lower energy pathway for the reaction and suggests that the evolutionary relationship between the two classes of cycloisomerases is more remote than previously believed.

The *3-cis,cis*-carboxymuconate cycloisomerases [EC 5.5.1.2; 2-carboxy-5-oxo-2,5-dihydrofuran-2-acetate lyase (decyclizing)] from *Pseudomonas putida* and *Acinetobacter calcoaceticus* catalyze the lactonization of 3-caraboxy-*cis,cis*-muconate (**1**) to yield 4-carboxymuconolactone (**2**).[2] This unusual reaction is a key step in the catabolism of protocatechuic acid, which, along with the battery of enzymes responsible for catechol catabolism, comprises the β-ketoadipate pathway (Scheme I).

[†] Yale-Celanese Fellow. University of Maryland and Yale University School of Medicine.
[‡] NIH Postdoctoral Fellow. University of Maryland.
[§] American Cancer Society Faculty Research Awardee. University of Maryland and Yale University School of Medicine. Address correspondence to this author at the University of Maryland.
[⊥] Department of Biology, Yale University.

(1) For a preliminary account of this work, see: Kozarich, J. W.; Chari, R. V. J.; Ngai, K.-L.; Ornston, L. N. In *Mechanisms of Enzymatic Reactions: Stereochemistry*; Frey, P. A., Ed.; Elsevier: New York, 1986; pp 233-246.
(2) (a) Ornston, L. N.; Stanier, R. Y. *J. Biol. Chem.* **1966**, *241*, 3776-3786. (b) Patel, R. N.; Meagher, R. B.; Ornston, L. N. *Biochemistry* **1973**, *12*, 3531-3537.

0002-7863/87/1509-5514$01.50/0